European Journal of Medicinal Chemistry 45 (2010) 4129–4139

Contents lists available at ScienceDirect

European Journal of Medicinal Chemistry

journal homepage: http://www.elsevier.com/locate/ejmech

Original article

Photodynamic effects of isosteric water-soluble phthalocyanines on human nasopharynx KB carcinoma cells

Julieta Marino [a,1], María C. García Vior [b,1], Lelia E. Dicelio [c], Leonor P. Roguin [a], Josefina Awruch [b,*]

[a] Instituto de Química y Fisicoquímica Biológicas (UBA-CONICET), Facultad de Farmacia y Bioquímica, Junín 956, 1113 Buenos Aires, Argentina
[b] Departamento de Química Orgánica, Facultad de Farmacia y Bioquímica, Universidad de Buenos Aires, Junín 956, 1113 Buenos Aires, Argentina
[c] INQUIMAE, Departamento de Química Inorgánica, Analítica y Química Física, Facultad de Ciencias Exactas y Naturales, Universidad de Buenos Aires, Ciudad Universitaria, Pabellón II, 1428 Buenos Aires, Argentina

ARTICLE INFO

Article history:
Received 13 January 2010
Received in revised form
7 May 2010
Accepted 2 June 2010
Available online 16 June 2010

Keywords:
Photodynamic therapy
Phthalocyanines
Singlet oxygen
Apoptosis
Lysosomes
KB cells

ABSTRACT

The photodynamic activity of water-soluble cationic zinc(II) phthalocyanines using human nasopharynx carcinoma (KB cells) was investigated. A sulfur-linked cationic dye, named: 2,9(10),16(17),23(24)-tetrakis [(2-trimethylammonium)ethylsulfanyl]phthalocyaninatozinc(II) tetraioidide (**13**) is the most active of four sensitizer assays and shows a singlet oxygen quantum yield of 0.58 and a higher bathochromic shift of 10 nm for the Q-band as compared with the oxygen-linked cationic aliphatic phthalocyanine: 2,9 (10),16(17),23(24)-tetrakis[(2-trimethylammonium)ethoxy]phthalocyaninatozinc(II) tetraioidide (**11**) and the best photo-stability in water in comparison with their tetra-α-substituted counterparts 1,8(11),15 (18),22(25)-tetrakis[(2-trimethylammonium)ethoxy]phthalocyaninatozinc(II) tetraioidide (**12**) and 1,8 (11),15(18),22(25)-tetrakis[(2-trimethylammonium)ethylsulfanyl]phthalocyaninatozinc(II) tetraioidide (**14**). Phthalocyanine **13**, partially localized in lysosomes, led to cell photoinactivation in a concentration- and light dose-dependent manner. After photodynamic treatment, compound **13** induced an apoptotic response – as indicated by morphological cell changes – an increase in the activity of caspase-3 and the cleavage of poly-ADP-ribose-polymerase substrate (PARP).

1. Introduction

Photodynamic therapy (PDT) is emerging as a promising method for the treatment of a variety of oncological, dermatological, cardiovascular and ophthalmic diseases [1–5]. PDT combines the intravenous or topical administration of a photosensitizer which preferentially localizes within the tumor, followed by illumination of the target tissue thus resulting in the formation of reactive oxygen species, believed to be responsible for the cascade of cellular and molecular events that finally lead to selective tumor destruction [1].

Phthalocyanines have been found to have applications as phototoxic drugs for PDT [4,6–8]. In addition to their well-known chemical stability, phthalocyanines possess characteristic absorption spectra [9], with a Soret band at approximately 350 nm and a usually narrow but very strong Q-band around 675 nm, with a molar absorption coefficient in the range of 10^5 M^{-1} cm^{-1}.

Zinc, aluminum, and silicon phthalocyanines that have been found to be useful photosensitizers for PDT, are efficient generators of singlet oxygen, the cytotoxic species capable of destroying malignant cells [10–14]. The silicon phthalocyanine Pc **4** is in various stages of clinical evaluation for cutaneous and subcutaneous lesions from diverse solid tumor origins [15].

The uptake and efficacy of photosensitizers such as phthalocyanines, porphyrins, and core-modified porphyrins are directly related to the number of hydrophilic groups [8,10] that the dye carries on its structure. Thus, in the aluminum sulfonate phthalocyanine series, those with two groups attached to the macrocycle show greater uptake and phototoxicity than phthalocyanines with three sulfonate groups which in turn show greater uptake and efficacy than phthalocyanines with four sulfonate groups. In BALB/c mice bearing EMT-6 tumors, aluminum sulfonate phthalocyanine substituted with two sulfonate groups is 10 times more phototoxic than aluminum phthalocyanine carrying four sulfonate groups [14]. Great efforts have been made to study the structure–activity relationship between the site [16,17] and kind of substitution [18] and the photodynamic activity. However, to our knowledge, studies directed to establish the structure–activity relationship between isosteric phthalocyanines are quite uncommon.

* Corresponding author. Tel.: +54 11 4964 8252; fax: +54 11 4508 3645.
E-mail address: jawruch@ffyb.uba.ar (J. Awruch).
[1] Both authors contributed equally to this work.

0223-5234/$ – see front matter © 2010 Elsevier Masson SAS. All rights reserved.
doi:10.1016/j.ejmech.2010.06.002

We herein report the photobiological studies of four isosteric water-soluble cationic zinc(II) phthalocyanines using human nasopharynx KB carcinoma cells. The properties of these phthalocyanines are compared and discussed in connection with their photophysical and photochemical evaluation. Our results show the efficiency of one of them: 2,9(10),16(17),23(24)-tetrakis[(2-trimethylammonium)ethylsulfanyl]phthalocyaninatozinc(II) tetraioidide (**13**) for suitable PDT applications. To further elucidate the cellular mechanism of action, we examined the intracellular localization for the purpose of determining the primary photodamage site. In addition, the prevailing mechanism of cell death after treatment was evaluated.

2. Results and discussion

2.1. Chemistry

In order to evaluate the effect of substitution on the efficacy of phthalocyanines, we synthesized cationic dyes **11**–**14**. The synthetic route is shown in Scheme 1; precursors **3**–**6** and phthalocyanines **7**–**14** were prepared by methods similar to those described in the literature with minor modifications [19–23]. Taking into account that the above phthalocyanines are for photophysical and photobiological studies, the synthesis of all compounds was described under Experimental Section. Briefly, phthalonitriles **3**–**6** were prepared by reaction of the corresponding commercially available 4- and 3-nitrophthalonitrile with the appropriate nucleophiles in the presence of potassium carbonate [19,24,25] in dry N,N-dimethylformamide (DMF) that is more effective than dimethylsulfoxide (DMSO) as the reaction solvent because it resulted in improved yields of pure products.

Phthalocyanines **7**–**8** were readily prepared by cyclotetramerization of phthalonitriles **3**–**4** employing 1,8-diazabicyclo [5.4.0]undec-7-ene (DBU) and zinc acetate at 150 °C whereas phthalocyanines **9**–**10** were prepared by reacting **5**–**6** with DBU and zinc acetate in butanol. Cationic phthalocyanines **11**–**14** were obtained by treatment of **7**–**10** with methyl iodide in methylene chloride. Intermediates **3**–**6** and dyes **7**–**14** were characterized by IR, ^{1}H NMR and ^{13}C NMR spectroscopy while EI-MS spectroscopy at 70 eV was performed for the characterization of **3**–**4**, o-dinitriles **5**–**6** ESI-MS spectroscopy was determined with a Micromass Ultima triple QUAD spectrometer since EI-MS at 70 eV or 40 eV only afforded decomposition fragments. Besides, ESI-TOF mass spectroscopy was employed for the characterization of phthalocyaninates **7**–**14**.

With regard to the solubility of phthalocyanines **7**–**10** they are soluble in almost all organic solvents, while cationic derivatives **11**–**14** are fully soluble in water and DMF.

2.2. Photophysical studies

The absorption spectra of zinc(II) phthalocyanines **11**–**14** in the 400–800 nm range are similar to those previously reported for other analogs in homogeneous media [26,27] (Fig. 1). Phthalocyanines **11**–**14** are strongly aggregated in water; their absorption spectra show an important dimer band blue-shifted even at low concentrations as shown in Fig. 1. This situation is reverted when DMF is employed as a solvent: the monomer band at *c.a.* 680 nm is enhanced and the dimer absorption becomes negligible.

The same behavior is evidenced by deviations of the Lambert–Beer law, in water (data not shown). The monomer spectra are similar to that reported for different zinc(II) phthalocyanines. On the other hand dimers are blue-shifted and different from the corresponding spectra of other phthalocyanines of the same family previously studied in our laboratory [26]. This agrees with the fact that, while dimer spectra of metallated phthalocyanines are dependent on the peripheral substituents and solvent polarity, that of the monomer remains practically unchanged [28].

Dyes were characterized by their photophysical properties; the Q-band of substituted 1, 8(11), 15(18), 22(25) (α) zinc(II) phthalocyanines **8**, **10**, **12** and **14** lie at a longer wavelength (14–20 nm) than 2,9(10),16(17),23(24) (β) derivatives **7**, **9**, **11** and **13** (Table 1). This red spectral shift is consistent with previous reports for substituted zinc(II) phthalocyaninates with electron-releasing groups [29,30] which can be reasonably explained by considering the extent of the atomic orbital coefficients of the carbon atoms derived from molecular orbital calculations. According to these authors since the coefficient of the α carbon atoms is larger than that of β carbon atoms in the HOMO, the destabilization extent of this orbital by introducing electron-donating groups is larger when said groups are linked to the α-positions, a fact that makes the HOMO–LUMO gap smaller and thereby results in the Q-band shifting to a longer wavelength [30].

A bathochromic shift of 10 nm is observed for the Q-bands when oxygen and sulfur are alternatively present. This effect was observed for phthalocyanines **7**–**10** and cationic derivatives **11**–**14** respectively [31,32]. Such bathochromic shift into the therapeutic window is highly promising for a second-generation photosensitizer for biomedical purposes in photodynamic therapy. Cationic

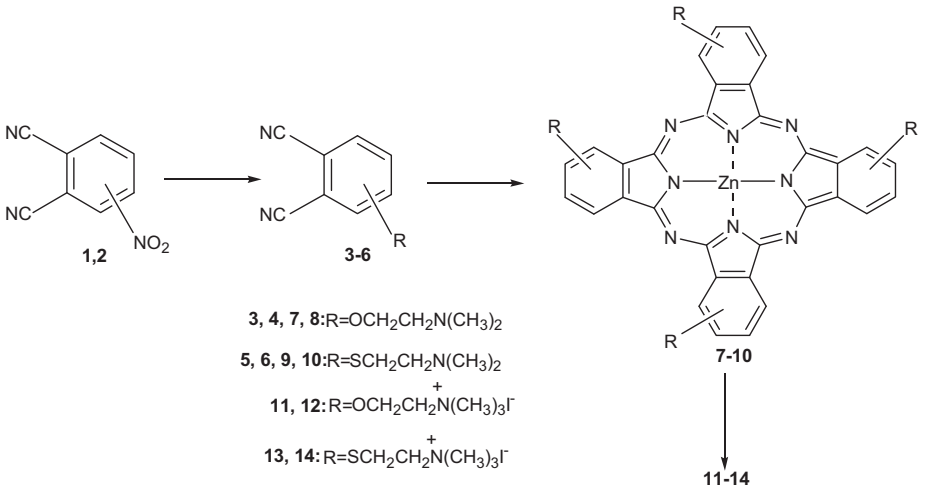

Scheme 1. Synthetic route to phthalocyanines **11**–**14**.

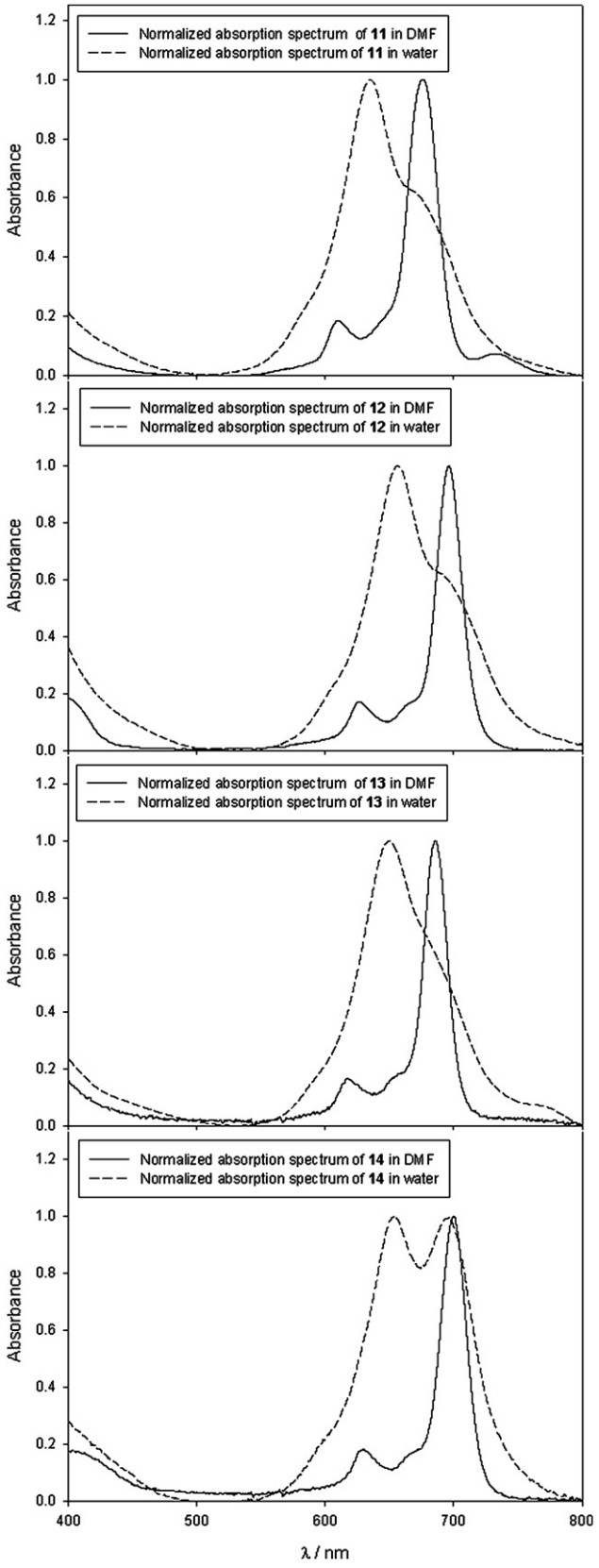

Fig. 1. Absorption spectra of **11**–**14** ——— 1×10^{-6} M in DMF and - - - - 5×10^{-7} M in water.

dimethylaminosulfanyl derivatives **13** and **14** present higher molar absorption coefficients (ε) in comparison with cationic dimethylaminoethoxy analogs **11** and **12**, this property improving skin light penetration (Table 1).

The emission spectra were similar in all solvents studied indicating that fluorescence can be attributed only to the monomer.

As previously reported [29,30] relative fluorescence quantum yields (Φ_F) are similar for compounds **7**, **9**, **11**, **13** and present higher Φ_F values than those of compounds **8**, **10**, **12**, **14**.

The quantum yield of singlet oxygen production (Φ_Δ) values obtained for dyes **7**–**14** are listed in Table 1. Sample absorbances were kept as low as possible to prevent aggregation yet enough to obtain measurable values of quantum yield of singlet oxygen production. Φ_Δ in homogeneous solution are similar to those previously published for lipophilic [26,33] as well as to cationic dyes [27] corresponding to zinc(II) phthalocyanine monomers at the concentration employed.

The photo-stability of **11**–**14** was analyzed in water by measuring the decrease in the Q-band over time irradiation with red light under air. The time decay of the absorbance maxima of the Q-band for all the compounds obeyed first-order kinetics as shown in Fig. 2.

The corresponding photodegradation constants *k* for phthalocyanines **7**–**14** are listed in Table 1. Lesser values of *k* mean a higher photo-oxidative stability. As shown in Table 1, tetra-β-substituted phthalocyanines **7**, **9**, **11** and **13** are more stable as compared with their tetra-α-substituted counterparts **8**, **10**, **12** and **14**. Moreover, the water solution of phthalocyanine **13** shows a lower value of *k* thus indicating it is more stable than **14** at the different irradiation times of our experiments and even in typical *in vitro* essays.

2.3. Photocytotoxicity studies

The effect of different concentrations of phthalocyanines **11**–**14** on KB cell survival was evaluated in the dark and upon exposure to a light dose of 4.7 J cm^{-2}, 1.96 mW cm^{-2} by employing the MTT assay. No dark cytotoxicity was observed when cells were exposed up to a 10 μM concentration of compounds **11**, **12** and **13** (Fig. 3A). On the contrary, when cells were treated with phthalocyanine **14**, cell viability diminished in a concentration-dependent manner, the 50% inhibition of cell proliferation (IC_{50}) being obtained at a concentration of 8 μM (Fig. 3A). After irradiation, **13** and **14** were found to be cytotoxic, and IC_{50} values from three independent experiments (mean ± SE) were 2.7 ± 0.6 μM and 0.8 ± 0.4 μM respectively (Fig. 3B). No effect on cell proliferation was observed after light exposure of KB cells previously incubated with phthalocyanines **11** and **12** (Fig. 3B). Since compound **14** diminished cell growth even in the absence of light, it was not further studied. The photocytotoxicity of **13** was also evaluated at different light doses. As shown in Fig. 3C, the efficacy of this phthalocyanine at a 10 μM concentration was light dose-dependent, decreasing cell viability by approximately 90% with a light dose of 4.7 J cm^{-2}.

It has been reported that cationic tetrasubstituted zinc(II) phthalocyanines containing the dimethylaminoethoxy group present photoredox activity on different malignant and non-malignant cell lines such as XP 29MAmal, CX1, HeLa, S180 and NO17 [34]; however, we have not detected, under our experimental conditions, any anti-tumoral activity for phthalocyanines with oxygen-linked cationic aliphatic chains (**11** and **12**).

In a recent manuscript [35] we stated that cultures of MCF-7c3 human breast cancer cells incubated with 2,3,9,10,16,17,23,24-octakis[(N,N-dimethylamino)ethylsulfanyl]phthalocyaninatozinc (II)-DMPC followed by a 27 J cm^{-2} irradiation dose led to a 70% inactivation at 0.5 μM whereas a substantially greater phototoxic effect was achieved at 1 μM which resulted in approximately 100% cell death.

Table 1
Photophysical parameters obtained for phthalocyanines **7**–**10** in THF and **11**–**14** in DMF and water and photodegradation constants *k* for **7**–**10** in THF and **11**–**14** in water.

Pc[a]	Solvent	Q_{band}	ε, λ_{max} M^{-1} cm^{-1}	Φ_F	Φ_Δ	*k* (10^{-3}.min^{-1})
7	THF	677	7.1×10^4	0.28 ± 0.02	0.61 ± 0.03	0.7
8	THF	697	7.7×10^4	0.19 ± 0.01	0.71 ± 0.02	2.3
9	THF	688	1.5×10^5	0.28 ± 0.03	0.60 ± 0.02	0.4
10	THF	706	1.9×10^5	0.18 ± 0.01	0.73 ± 0.02	1.8
11	DMF	676	1.1×10^5	0.15 ± 0.01	0.69 ± 0.02	–
	Water	635, 674	6.2×10^4 (674 nm)[b]	0.08 ± 0.01	0.57 ± 0.02	3.0
12	DMF	696	1.2×10^5	0.09 ± 0.01	0.73 ± 0.03	–
	Water	657, 694	6.6×10^4 (694 nm)[b]	0.07 ± 0.01	0.56 ± 0.02	41
13	DMF	686	1.8×10^5	0.15 ± 0.01	0.71 ± 0.03	–
	Water	649, 684	5.8×10^4 (684 nm)[b]	0.09 ± 0.01	0.58 ± 0.02	9.0
14	DMF	700	2.2×10^5	0.07 ± 0.01	0.76 ± 0.02	–
	Water	653, 696	1.4×10^5 (696 nm)[b]	0.06 ± 0.01	0.62 ± 0.02	23

[a] Experiments were carried out in concentrations ranging between 1×10^{-7} M and 6×10^{-6} M for **7**–**10** in THF and **11**–**14** in DMF and between 5×10^{-8} M and 5×10^{-7} M for **11**–**14** in water.
[b] ε_{app} at the monomer band.

2.4. Cellular uptake of phthalocyanine *13* in KB cells

The uptake of a 10 μM solution of **13** was measured after incubating KB cells for different time-periods in the dark. As shown in Fig. 4A, a rapid significant uptake of **13** was observed after 30 min exposure, reaching a plateau after 4 h. A cytosolic localization of **13** with a typical red fluorescence emission was observed by confocal microscopy after 24 h incubation by exciting at 633 nm and detecting the emission fluorescence at wavelengths >660 nm (Fig. 4B). Cellular uptakes of compounds **11** and **12** were not determined due to the absence of photocytotoxicity.

2.5. Intracellular localization of phthalocyanine *13*

The subcellular localization of **13** was evaluated by confocal microscopy after incubating KB cells for 24 h in the dark and staining them with fluorescent dyes for specific organelles. As shown in Fig. 5A, compound **13** – mainly found in the cytoplasmic region – co-localized with the green fluorescence of the specific lysosome probe. Thus, yellow vesicles were visualized from the overlay of the red fluorescence from **13** and LysoTracker signals. When MitoTracker Green was employed as a mitochondria fluorescent probe, it was found that compound **13** did not show a mitochondrial localization, since no overlapping of red and green signals was observed (Fig. 6A).

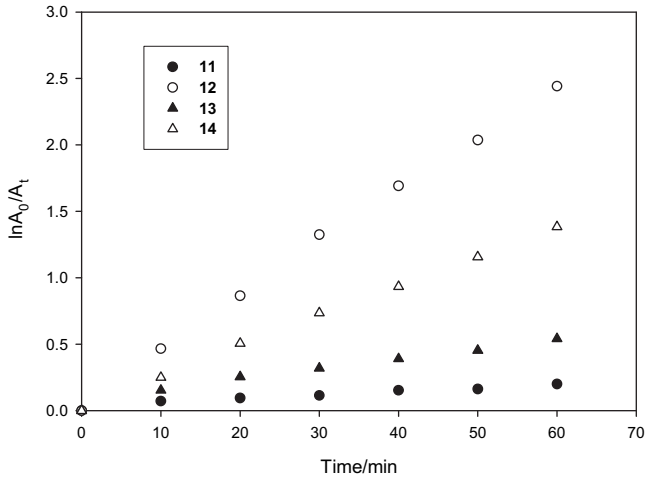

Fig. 2. First-order plots for the photodegradation of phthalocyanines **11**–**14** in water.

The cellular uptake of phthalocyanines and related macrocycles is known to depend on their hydrophobic character, overall charge and charge distribution [36]. Thus, meso-tetraphenylporphyrin derivatives bearing adjacent 5,15-di[4-(N-trimethylaminophenyl)-15,20-diphenylporphyrin] (DADP-a) or opposite 5,10-di[4-(N-trimethylaminophenyl)-10,20-diphenylporphyrin] (DADP-o) cationic N-$(CH_3)_3^+$ groups on two of the para-phenyl positions were examined for photodynamic properties as a function of charge distribution. DADP-a selectively binds to mitochondria whereas DADP-o which has a different charge distribution, showed lysosomal affinity [37]. This property is shown by other sensitizers including the chlorin NPe6 and the lutetium texaphyrin [38] since symmetrical cationic phthalocyanine with either Zn(II) or Si(IV) metal ions localized preferentially within the cell lysosomes [36]. Fluorescence images were also examined 3 h after irradiation. Under these conditions, the punctuate pattern of the lysosomal probe was less evident and no difference in mitochondrial labeling was detected thus suggesting a possible lysosomal membrane permeabilization (Figs. 5B and 6B). In addition, characteristic morphological changes of apoptotic cells such as cell shrinkage and membrane blebbing, were observed [39,40]. By using Hoechst 33258-staining, apoptotic condensed and fragmented nuclei were also evident 3 h and 24 h after irradiation of KB cells incubated with compound **13** (Fig. 7). A nuclear localization of **13** was also detected, probably due to the alteration of the nuclear membrane permeability (Figs. 5B and 6B).

2.6. Evaluation of apoptosis mediated by phthalocyanine *13*

It is well-known that the apoptosis is mediated by the activation of aspartate specific cysteine proteases named caspases [39–44]. Activation of the initiator caspases-8 and -9 leads to the cleavage of effector caspases such as caspase-3 which cleaves most cellular substrates responsible for the typical morphological and biochemical changes that occur during apoptosis. In order to evaluate the induction of an apoptotic response mediated by caspase activation, we measured the proteolytic activity of the executioner caspase-3. As shown in Fig. 8, a slight increase in caspase-3 activity was observed 1 h after light exposure of KB cells preloaded with phthalocyanine **13**. This activity reached a peak after 3 h and remained high up to 24 h post-irradiation. No effect on caspase activation was found in non-irradiated KB cells with or without **13** or irradiated cells in the absence of **13**. We also determined the ability of caspase-3 to hydrolyze PARP (Poly-ADP-Ribose-Polymerase). PARP, a 113 kDa protein that binds and repairs DNA strand breaks, is also a substrate for caspase-3 [45–47]. Thus, a fragment of 89 kDa, unable to repair DNA damage originated

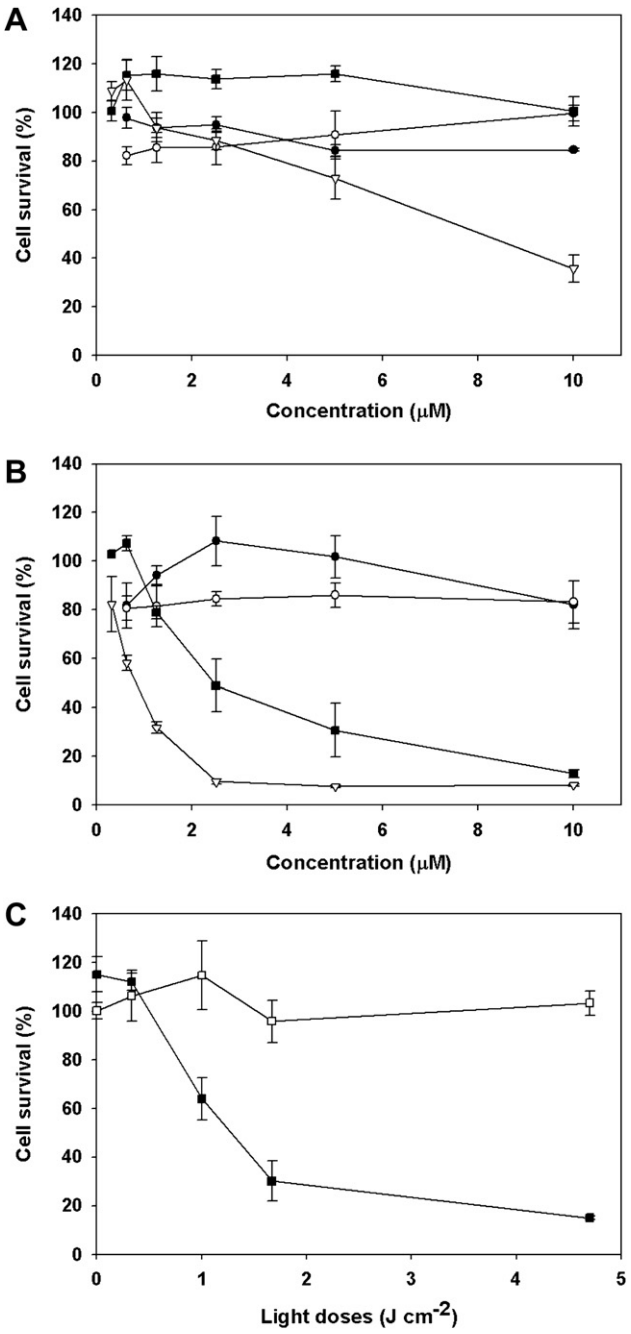

Fig. 3. Effect of phthalocyanines **11**–**14** on KB cell viability. (A) Different concentrations of **11** (●), **12** (○), **13** (■) and **14** (▽) were incubated with KB cells in the dark or (B) were exposed to a light dose of 4.7 J cm^{-2}. (C) Cells preloaded with 10 μM of **13** (■) were irradiated with various light doses. Control cells without **13** (□) were kept in the dark. The MTT cytotoxicity assay was carried out 24 h after treatment as described under Materials and methods. Results are expressed as the percentage of growth obtained in the absence of phthalocyanines (control) and represent the mean ± S.E. of three different experiments.

during apoptosis, is obtained after proteolysis of PARP. Western blot assays were performed to evaluate caspase-3-mediated PARP cleavage (Fig. 9). A similar significant increase in cleaved PARP (89 kDa fragment) was shown 3 h and 24 h after light exposure of cells preloaded with **13**. As controls, no effect on PARP cleavage was observed in non-irradiated KB cells with or without **13** or irradiated cells in the absence of **13**. The intracellular localization of phthalocyanines or other compounds in lysosomes could contribute to trigger an apoptotic cell death pathway [37,48,49]. Our results suggest that Pc **13** induced-apoptotic response mediated by caspase-3 activation could be downstream a lysosomal event. Thus, as previously reported, a partial lysosomal membrane permeabilization and the consequent release of proteolytic enzymes into cytosol lead to a lysosomal pathway of apoptosis which is connected to mitochondrial dysfunction and caspase activation [50–52].

3. Conclusions

The study herein investigates some biophysical aspects and the *in vitro* photodynamic effects of a tetrasubstituted zinc(II) phthalocyanine replaced with sulfur-linked cationic aliphatic chains in a human nasopharynx carcinoma cell line.

This water-soluble cationic phthalocyanine **13** was selected from a panel of four analogs of oxygen- and sulfur-linked cationic aliphatic isosteric compounds showing a Φ_Δ of 0.58, a higher bathochromic shift of 10 nm for the Q-band as compared with oxygen-linked aliphatic phthalocyanine **11** and also the best photostability in water as compared with their tetra-α-substituted counterparts **12** and **14**. The above shift into the therapeutic window observed for **13** is an asset for biomedical applications in photodynamic therapy. Besides, cationic dimethylaminosulfanyl derivatives **13** and **14** present higher values of molar absorption coefficients (ε) in comparison with cationic dimethylaminoethoxy analogs **11** and **12**, this property improving skin light penetration. Additionally, phthalocyanine **13** had no dark toxicity as compared with its isomer **14** and showed an effective photodynamic activity in KB cells which agrees with our previous finding about the photodynamic efficiency of sulfur-linked zinc(II) phthalocyanines [33]. This dye localized subcellularly within the lysosomes and triggered after irradiation lysosomal-induced apoptosis leading to a 90% cell death.

The above results have prompted us to consider performing *in vivo* studies of **13**.

4. Experimental

4.1. Materials and methods

4.1.1. Synthesis of photosensitizers

Melting points were determined on an Electrothermal 9100 capillary melting point apparatus. ^{1}H NMR and ^{13}C NMR were recorded on a Bruker MSL 300 spectrometer. ^{1}H NMR and ^{13}C NMR of phthalocyanines were recorded on a Bruker AM 500. Mass spectra were obtained with a TRIO 2 (electronic ionization 70 eV) spectrometer. Phthalocyanines ESI mass spectra were measured with a Q-TOF Premier micromass/Waters Corporation spectrometer. Electronic absorption spectra were determined with a Shimadzu UV-3101 PC spectrophotometer. Fluorescence spectra were monitored with a QuantaMaster Model QM-1 PTI spectrofluorometer. Infrared spectra were performed with a Perkin Elmer Spectrum One FT-IR spectrometer.

Chromatography columns were prepared with TLC Kiesegel (Merck), and Aluminum Oxide 90 standardized (Merck). N,N-dimethylformamide was dried over 3 Å molecular sieves during 72 h, then filtered and freshly distilled before utilization [53]. Diphenylisobenzofuran (DPBF), N,N-diethyl-4-nitrosoaniline, imidazol and Methylene blue (MB) as well as all reagents were provided by Sigma–Aldrich. Tetra-*t*-butylphthalocyaninatozinc(II) [26], 2,3,9,10,16,17,23,24-octakis(decyloxi)phthalocyaninatozinc(II) (ZnPc) [33] and 2,3,9,10,16,17,23,24-octakis[(N,N-dimethylaminoethylsulfanyl)]phthalocyaninatozinc(II) [31] were synthesized in our laboratory.

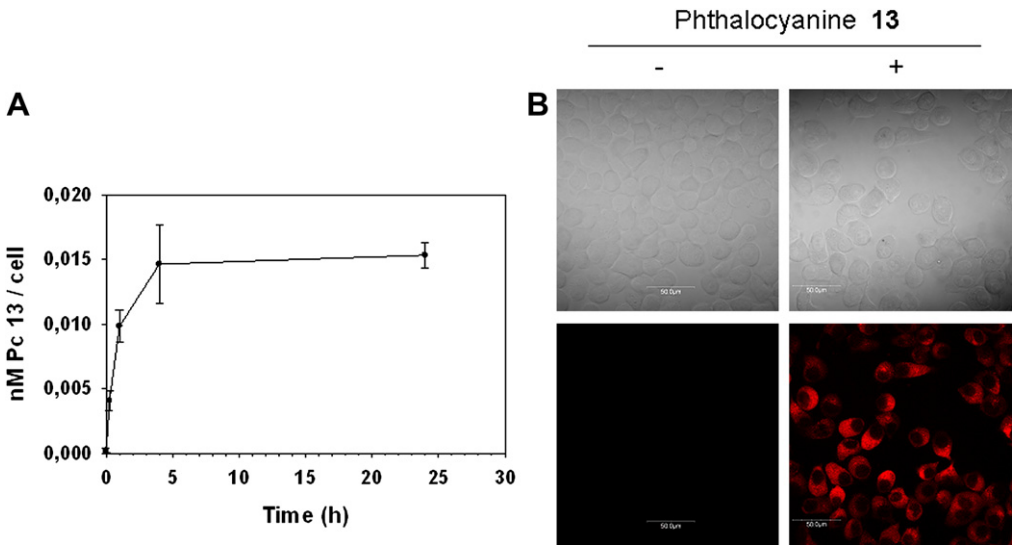

Fig. 4. Time-dependent uptake of phthalocyanine **13**. (A) KB cells were incubated for different time-periods in the dark with a 10 μM concentration of **13**. (B) Intracellular localization of **13** was visualized by confocal microscopy after incubating KB cells for 24 h in the dark. The upper panel corresponds to phase contrast and lower panel to fluorescence images.

*4.1.2. 1,2-Dicyano-4-[2-(N,N-dimethylamino)ethoxy]benzene (**3**) [19,34]*

A mixture of 2-dimethylaminoethanol (0.30 mL, 2.983 mmol) and K_2CO_3 (0.608 g, 4.4 mmol) in DMF (3 mL) was stirred under argon at room temperature for 2 h and 4-nitrophthalonitrile (**1**) (0.100 g, 0.58 mmol) was added and stirring continued for another 96 h. The reaction mixture was poured into water (50 mL) and extracted with CH_2Cl_2 (3 × 30 mL) and the combined extracts were washed with water (3 × 30 mL) and dried over Na_2SO_4. After evaporation in vacuo, the residue was dissolved in a small volume

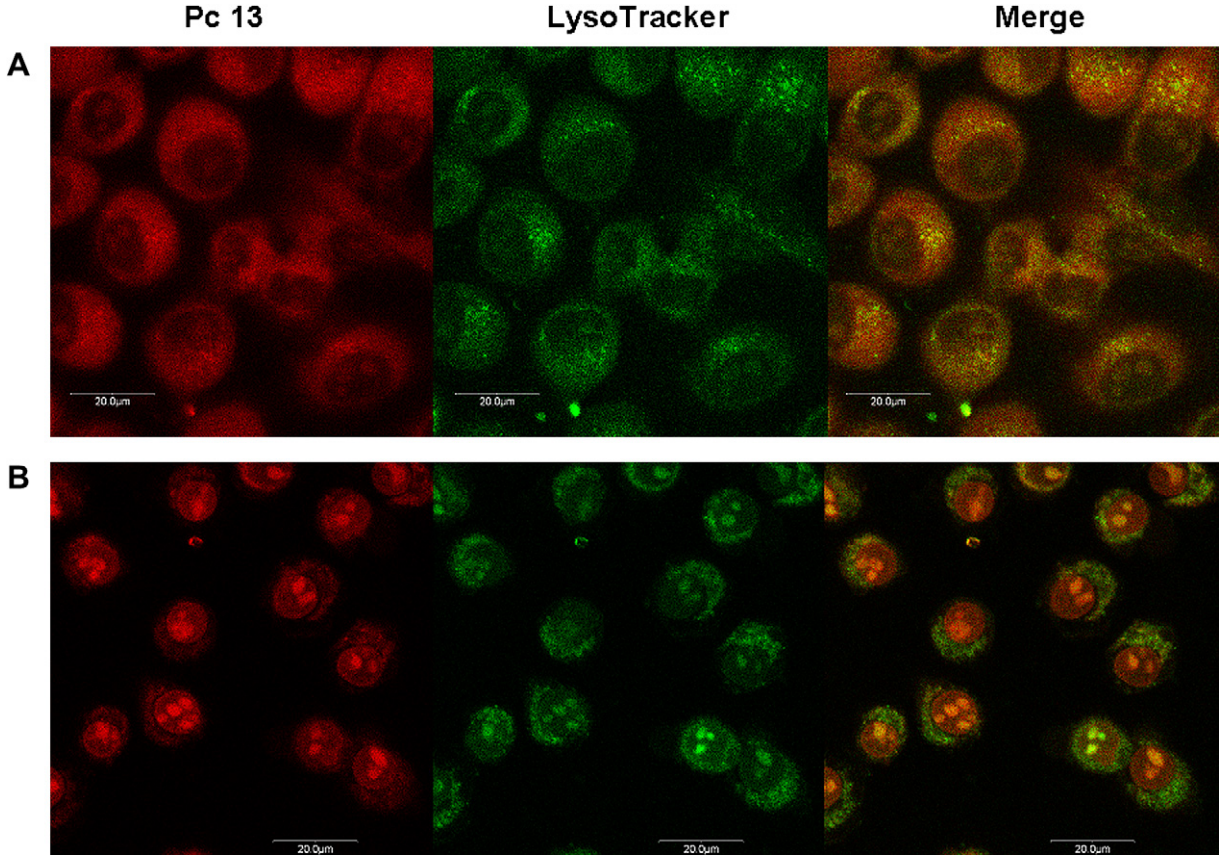

Fig. 5. Co-localization of **13** with lysosomes. KB cells incubated with 10 μM of **13** for 24 h were stained with LysoTracker Green DND-26 (75 nM, 30 min) and kept in the dark (A) or exposed to a 4.7 J cm^{-2} light dose and then incubated for an additional 3 h (B). Red fluorescence corresponds to **13** and green fluorescence represents the signal for LysoTracker Green.

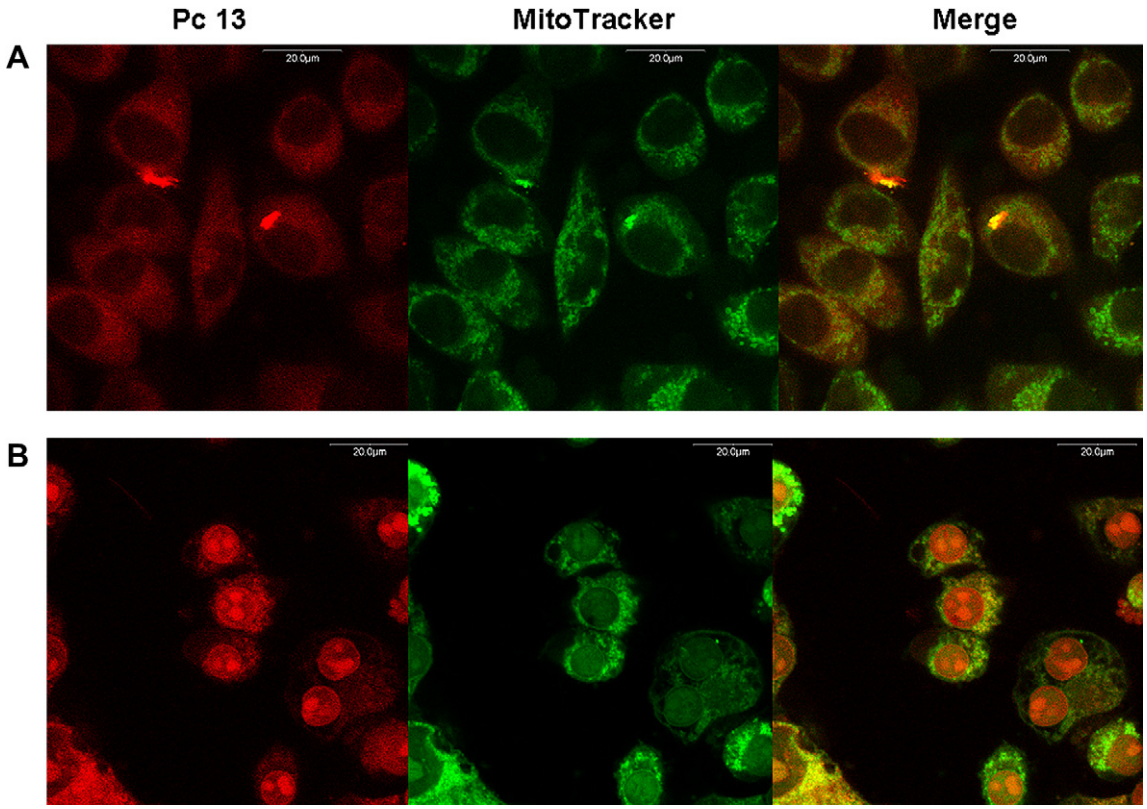

Fig. 6. Intracellular localization of **13** and mitochondria staining. KB cells incubated with 10 μM of **13** for 24 h were stained with MitoTracker Green FM (100 nM, 45 min) and kept in the dark (A) or exposed to a 4.7 J cm^{-2} light dose and then incubated for an additional 3 h (B). Red fluorescence corresponds to **13** and green fluorescence represents the signal for MitoTracker Green.

of CH_2Cl_2-MeOH (95:5) and filtered through a silica–gel column packed and pre-washed with the same solvent. After evaporation of the solvent, an oil was obtained. Yield: 0.110 g (89%). IR (KBr, cm^{-1}): 3065, 3030, 2967, 2235 (CN), 1599, 1562, 1494, 1473, 1310, 1293, 1257, 1182, 1104, 1033, 905, 858, 724, 642, 525, 462. ^{1}H NMR (300 MHz, $CDCl_3$): δ (ppm) 2.47(s, 6H, CH_3), 2.93 (t, 2H, $J = 5.13$ Hz, CH_2N), 4.26 (t, 2H, $J = 5.13$ Hz, OCH_2), 7.24 (d, 1H, $J = 6.15$ Hz, Ar), 7.30 (s, 1H, Ar), 7.72 (d, 1H, $J = 8.72$ Hz, Ar). ^{13}C NMR: δ (ppm) 45.35, 58.02, 64.83, 106.82, 112.67, 115.30, 117.19, 119.78, 120.46, 135.13, 163.21. MS (EI, 70 eV): m/z (%) 215 (1.94) [M^+], 216 (4.12) [$M^+ + 1$], 58 (100). Anal. Calcd. for $C_{12}H_{13}N_3O$: C, 66.96; H, 6.09; N, 19.52. Found; C, 67.03; H, 6.06; N, 19.60.

4.1.3. 1,2-Dicyano-3-[2-(N,N-dimethylamino)ethoxy]benzene (**4**) [19]

A mixture of 3-nitrophthalonitrile (**2**) (0.100 g, 0.58 mmol), 2-dimethylaminoethanol (0.30 mL, 2.983 mmol), K_2CO_3 (0.608 g, 4.4 mmol) in DMF (3 mL) was reacted by applying the procedure described for **3**. An oil was obtained. Yield: 0.106 g (85%). IR (KBr, cm^{-1}): 3000, 2229 (CN), 1662, 1583, 1473, 1345, 1289, 1062, 795,729. ^{1}H NMR (300 MHz, $CDCl_3$): δ (ppm) 2.67(s, 6H, CH_3), 3.19 (t, 2H, $J = 5.13$ Hz, CH_2N), 4.51 (t, 2H, $J = 5.13$ Hz, OCH_2), 7.29 (d, 1H, $J = 8.72$ Hz, Ar), 7.40 (d, 1H, $J = 7.7$ Hz, Ar), 7.67 (t, 1H, $J = 7.95$ Hz, Ar). ^{13}C NMR: δ (ppm) 45.41, 57.92, 68.04, 101.68, 113.03, 116.31, 116.52, 120.90, 127.18, 134.11, 164.14. MS (EI, 70 eV): m/z (%) 214 (0.66) [$M^+ - 1$], 58 (100). Anal. Calcd. for $C_{12}H_{13}N_3O$: C, 66.96; H, 6.09; N, 19.52. Found: C, 66.90; H, 6.07; N, 19.62.

4.1.4. 1,2-Dicyano-4-[2-(N,N-dimethylamino)ethylsulfanyl]benzene (**5**) [20–22]

A mixture of 2-(dimethylamino)ethanethiol hydrochloride (0.123 g, 0.867 mmol) and K_2CO_3 (0.608 g, 4.4 mmol) in DMF (3 mL) was stirred under argon at room temperature for 2 h and 4-nitrophthalonitrile (**1**) (0.100 g, 0.58 mmol) was reacted by applying the

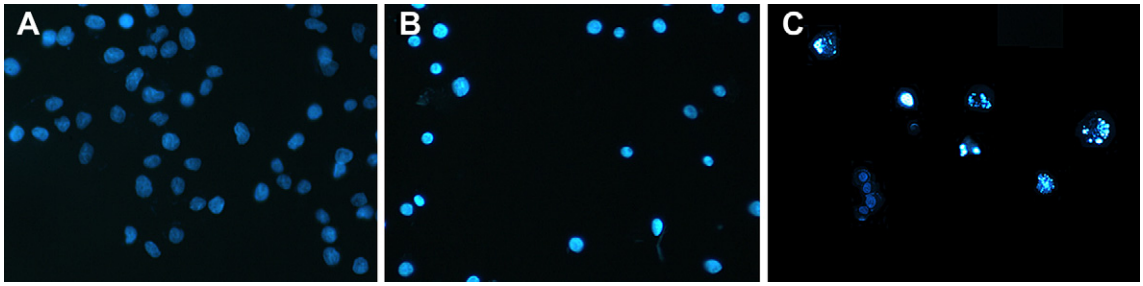

Fig. 7. Morphological changes visualization by Hoechst 33258-staining. KB cells incubated with 5 μM of **13** were stained 3 h (B) and 24 h (C) after irradiation with Hoechst 33258. Non-irradiated cells (control) are shown in panel A. (Magnification 400×).

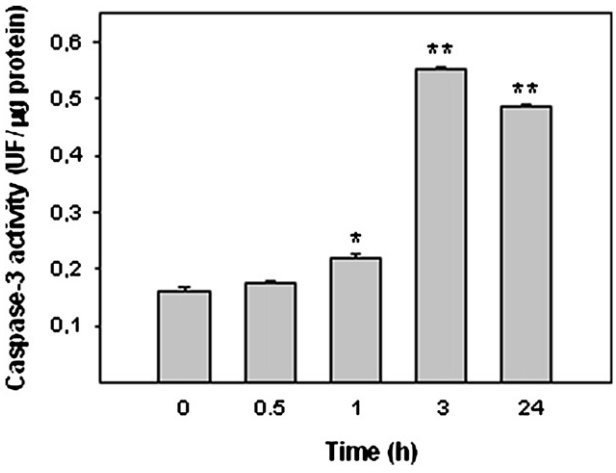

Fig. 8. Caspase-3 activation after irradiation. KB cells preloaded with 5 μM of **13** were irradiated with a light dose of 4.7 J cm^{-2} and incubated for different time-periods. Cells irradiated without **13** and incubated during the same periods were used as controls. Since similar results were obtained, only the control value corresponding to time 0 is shown. Caspase-3 activity was determined as indicated in Materials and methods. Enzymatic activity is expressed as the fluorescence per μg of protein and represents the mean values ± SE of three different experiments. Statistical significance in comparison with the corresponding control is indicated by $^{*}p < 0.01$ or $^{**}p < 0.0001$.

procedure described for **3**. A solid residue was obtained that was recrystallized from ethanol. Yield: 0.081 g (60%); mp 125–127 °C. IR (KBr, cm^{-1}): 2991, 2963, 2926, 2881, 2854, 2742, 2483, 2342, 2256, 2241(CN), 1981, 1842, 1793, 1736, 1610, 1534, 1357, 1298, 1263, 1179,1076, 924, 871, 801, 745, 600, 525, 489. ^{1}H NMR (300 MHz, $CDCl_3$): δ (ppm) 2.31(s, 6H, CH_3), 2.65 (t, 2H, $J = 6.75$ Hz, CH_2N), 3.14 (t, 2H, $J = 6.75$ Hz, SCH_2), 7.51 (dd, 1H, $J = 8.22$, 1.76 Hz, Ar), 7.58 (d, 1H, Ar), 7.64 (d, 1H, $J = 8.22$ Hz, Ar). ^{13}C NMR: δ (ppm) 30.71, 44.65, 58.30, 113.08, 114.72, 115.29, 115.38, 132.70, 136.46, 136.62, 141.83. ESI-TOF MS: *m/z* (%) 232.2 (100)[$M^+ + 1$], 233.2 (16.1) [$M^+ + 2$]. Anal. Calcd. for $C_{12}H_{13}N_3S$: C, 62.31; H, 5.66; N, 18.17. Found: C, 62.48; H, 5.69; N, 18.25.

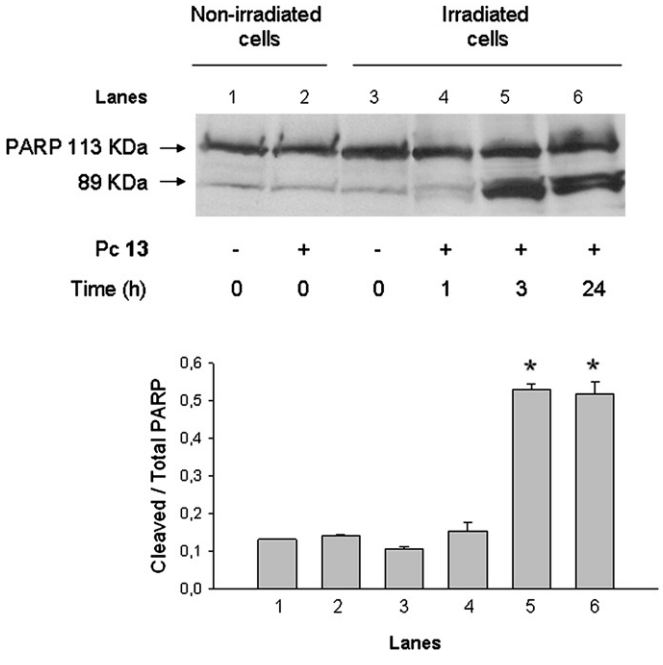

Fig. 9. PARP cleavage after PDT. KB cells with 5 μM of **13** were exposed to a light dose of 4.7 J cm^{-2}, incubated for different time-periods and then submitted to Western blot assays as described under Materials and methods (lanes 4–6). Non-irradiated cells with or without **13** (lanes 1 and 2 respectively) or irradiated cells without **13** (lane 3) were used as controls. Densitometric analyses show the relationship of the 89 kDa fragment with regard to the total amount of PARP. Results are expressed as the mean ± SE of three different experiments ($^{*}p < 0.0001$).

*4.1.5. 1,2-Dicyano-3-[(2-N,N-dimethylamino)ethylsulfanyl]benzene (**6**) [21,22]*

A mixture of 2-(dimethylamino)ethanethiol hydrochloride (0.123 g, 0.867 mmol) and K_2CO_3 (0.608 g, 4.4 mmol) in DMF (3 mL) was reacted by applying the procedure described for **3**. A white solid was obtained that was recrystallized from ethanol. Yield: 0.074 g (55%); mp 94 °C. IR (KBr, cm^{-1}):2969, 2943, 2862, 2824, 2792, 2777, 2229 (CN), 1989, 1812, 1702, 1566, 1452, 1421, 1407, 1377, 1303, 1289, 1269, 1253, 1229, 1196, 1156, 1100, 1067, 1042, 1011, 963, 903, 856, 797, 785, 727, 698, 621, 583, 552, 537, 499. ^{1}H NMR ($CDCl_3$, 300 MHz): δ (ppm) 2.28(s, 6H, CH_3),2.63 (t, 2H, $J = 7.18$ Hz, CH_2N), 3.17 (t, 2H, $J = 7.18$ Hz, SCH_2), 7.55 (dd, 1H, $J = 6.93$, 2.31 Hz, Ar), 7.61 (s, 1H, Ar), 7.63 (d, 1H, $J = 6.93$ Hz, Ar). ^{13}C NMR: δ (ppm) 33.89, 44.54, 58.27, 113.20, 114.72, 115.33, 115.62, 123.65, 131.45, 132.10, 138.28. ESI-TOF MS: *m/z* (%) $[M + H]^+$ cald for: $C_{12}H_{13}N_3S$ 232.0902; found: $[M + H]^+$ 232.0903. Anal. Calcd. for $C_{12}H_{13}N_3S$: C, 62.31; H, 5.66; N, 18.17. Found: C, 62.39; H, 5.64; N, 18.28.

*4.1.6. 2,9(10),16(17),23(24)-Tetrakis[(2-dimethylamino)ethoxy] phthalocyaninatozinc(II) (**7**) [23,34]*

A mixture of **3** (0.030 g, 0.139 mmol), anhydrous zinc acetate (0.030 g, 0.137 mmol), and DBU (0.1 mL, 0.67 mmol) was stirred and heated at 150 °C under argon during 1 h. The mixture was cooled down and 5 mL of CH_2Cl_2 was added, and centrifuged to eliminate the excess of zinc acetate. The methylene chloride solution was washed with water (3 × 5 mL) and evaporated in vacuo. The blue-green solid was then applied to an aluminum oxide column packed and pre-washed with CH_2Cl_2. After washing with CH_2Cl_2, the title compound was eluted with CH_2Cl_2-methanol (98:2) and evaporated. The dye was recrystallized from CH_2Cl_2–hexane. Yield 0.027 g (85%). IR (KBr, cm^{-1}): 2930, 1648, 1514, 1471, 1390, 1220, 1172, 1098, 832, 758. ^{1}H NMR (500 MHz, $CDCl_3$): δ(ppm) 3.35 (br s, 24H, CH_3), 4.10 (m, 8H, CH_2N), 4.65 (m, 8H, OCH_2), 6.75–7.70 (m, 12H, Ar). ^{13}C NMR: δ (ppm) 45.05, 57.85, 64.35, 74.50, 108.23, 116.37, 121.22, 124.51, 136.44, 142.13, 161.73. ESI-TOF MS: *m/z* [M^+] calcd. for $C_{48}H_{52}N_{12}O_4Zn$: 926.4094; found: [M^+] 926.3523 and [$M^+ + 1$] 927.3526.

*4.1.7. 1,8(11),15(18),22(25)-Tetrakis[(2-dimethylamino)ethoxy] phthalocyaninatozinc(II) (**8**) [22]*

A mixture of **4** (0.040 g, 0.186 mmol), anhydrous zinc acetate (0.040 g, 0.182 mmol), and DBU (0.1 mL, 0.67 mmol) was reacted by applying the procedure described for **7**. The dye was recrystallized from CH_2Cl_2-hexane. Yield 0.031 g (73%). IR (KBr, cm^{-1}): 2925, 1651, 1513, 1470, 1351, 1234, 1213, 1079, 831, 757. ^{1}H NMR (500 MHz, $CDCl_3$): δ (ppm) 2.34 (br s, 24H, CH_3), 2.89 (m, 8H, CH_2N), 3.82 (m, 8H, OCH_2), 6.70–7.87 (m, 12H, Ar). ^{13}C NMR: δ (ppm) 45.52, 58.02, 65.26, 75.32, 81.73, 115.62, 121.41, 125.78, 130.65, 150.56, 159.84, 164.11, 176.70. ESI-TOF MS: *m/z* [M^+] calcd. for $C_{48}H_{52}N_{12}O_4Zn$: 926.4094; found: [M^+] 926.3655 and [$M^+ + 1$] 927.3655.

*4.1.8. 2,9(10),16(17),23(24)Tetrakis[(2-dimethylamino) ethylsulfanyl]phthalocyaninatozinc(II) (**9**) [20–22]*

A mixture of **5** (0.050 g, 0.216 mmol), anhydrous zinc acetate (0.050 g, 0.225 mmol), and DBU (0.2 mL, 1.34 mmol) in anhydrous butanol (4 mL) was stirred and heated at reflux temperature for 1 h under argon. After evaporation in vacuo, the residue was treated with methylene chloride (5 mL) and cooled during 24 h. After centrifugation to eliminate the excess of zinc acetate, the solution

was evaporated in vacuo leaving a blue solid, that was then applied to an aluminum oxide column packed and pre-washed with CH_2Cl_2. After washing with CH_2Cl_2, the title compound was eluted with CH_2Cl_2-methanol (98:2) and evaporated. The dye was recrystallized from CH_2Cl_2-hexane. Yield 0.048 g (89%). IR (KBr, cm^{-1}): 2928, 1645, 1514, 1468, 1200, 1098, 1042, 958, 831, 758. ^1H NMR (500 MHz, $CDCl_3$): δ (ppm) 1.61 (br s, 24H, CH_3), 2.55 (m, 8H, CH_2N), 3.37 (m, 8H, SCH_2), 6.80–7.80 (m, 12H, Ar). ^{13}C NMR: δ (ppm) 30.88, 44.91, 58.73, 121.05, 126.16, 128.59, 134.32, 139.73, 150.18, 165.25, 170.62. ESI-TOF MS: m/z [M^+] calcd. for $C_{48}H_{52}N_{12}S_4Zn$: 990.6757; found: [M^+] 990.2611 and [$M^+ + 1$] 991.2610.

4.1.9. 1,8(11),15(18),22(25)-Tetrakis[(2-dimethylamino) ethylsulfanyl]phthalocyaninatozinc(II) (**10**) [21,22]

A mixture of 5 (0.050 g, 0.216 mmol), anhydrous zinc acetate (0.050 g, 0.225 mmol), and DBU (0.2 mL, 1.34 mmol) in anhydrous butanol (4 mL) was stirred and heated at reflux temperature for 2 h under argon, following by the procedure described for **9**. The dye was recrystallized from CH_2Cl_2-hexane. Yield 0.038 g (70%). IR (KBr, cm^{-1}): 2922, 2851,1622, 1459, 1385, 1315, 1261, 1107, 897, 798, 758, 742, 618. ^1H NMR (500 MHz, $CDCl_3$): δ (ppm) 2.30(bs, 24H, CH_3), 2.65 (m, 8H, CH_2N), 3.24 (m, 8H, SCH_2), 7.10–7.83 (m, 12H, Ar). ^{13}C NMR: δ (ppm) 31.62, 44.38, 58.71, 75.84, 122.59, 128.03, 133.13, 147.10, 159.23, 165.79, 172.15. ESI-TOF MS: m/z [M^+] calcd. for $C_{48}H_{52}N_{12}S_4Zn$: 990.2614; found [M^+] 990.2596 and [$M + H]^+$ 991.2610.

4.1.10. 2,9(10),16(17),23(24)-Tetrakis[(2-trimethylammonium) ethoxy]phthalocyaninatozinc(II) tetraioidide (**11**) [22,23,34]

Methyl iodide (3 mL, 48 mmol) was added to a solution of phthalocyanine **7** (0.02 g, 0.013 mmol) in methylene chloride (5 mL) and the solution was stirred for 48 h at 60 °C. After cooling to room temperature, the blue-green powder was centrifuged, dissolved in methanol and precipitated with methylene chloride, and centrifuged again. Yield 0.031 g (95%). IR (KBr, cm^{-1}): 2922, 1608, 1489, 1338, 1231, 1097, 968, 746. ^1H NMR (DMSO-d_6, 500 MHz): δ (ppm) 3.38 (br s, 36H, CH_3), 4.15 (m, 8H, CH_2N), 4.69 (m, 8H, OCH_2), 7.15–7.78 (m, 12H, Ar). ^{13}C NMR: δ (ppm) 54.91, 64.53, 66.15, 109.12, 117.19, 124.61, 133.17, 149.76, 160.29, 163.18, 171.03. ESI-TOF MS: m/z [M^+] calcd for $C_{52}H_{64}N_{12}O_4I_4Zn$: 1494.0647; found [$M^+$] 1494.0723.

4.1.11. 1,8(11),15(18),22(25)-Tetrakis[(2-trimethylammonium) ethoxy]phthalocyaninatozinc(II) tetraioidide (**12**) [22]

This compound was prepared from **8** by applying the procedure described for **11**. Yield 0.030 g (90%). IR (KBr, cm^{-1}): 2929, 1706, 1614, 1488, 1265, 1203, 1088, 979, 951,881, 805, 747. ^1H NMR (DMSO-d_6, 500 MHz): δ (ppm) 2.38 (br s, 36H, CH_3), 3.02 (m, 8H, CH_2N), 3.99 (m, 8H, OCH_2), 6.87–8.02 (m, 12H, Ar). ^{13}C NMR: δ (ppm) 54.90, 66.12, 109.25, 114.38, 116.30, 120.28, 126.63, 131.49, 150.05, 157.07, 165.29, 171.17, 176.72. ESI-TOF MS: m/z [M^+] calcd for $C_{52}H_{64}N_{12}O_4I_4Zn$: 1494.0647; found [$M^+$] 1494.0723.

4.1.12. 2,9(10),16(17),23(24)-Tetrakis[(2-trimethylammonium) ethylsulfanyl]phthalocyaninatozinc(II)tetraioidide (13) [20–22]

Methyl iodide (3 mL, 48 mmol) was added to a solution of phthalocyanine **9** (0.03 g, 0.019 mmol) in methylene chloride (5 mL) and the solution was stirred for 48 h at 60 °C. After cooling to room temperature, the blue-green powder was centrifuged, dissolved in methanol and precipitated with methylene chloride, and centrifuged again. Yield 0.046 g (97%). IR (KBr, cm^{-1}): 2929, 1618, 1474, 1401, 1384, 1128, 605. ^1H NMR (DMSO-d_6, 500 MHz): δ (ppm) 3.37 (br s, 36H, CH_3), 4.21 (m, 8H, CH_2N), 4.67 (m, 8H, SCH_2), 7.23–7.87 (m, 12H, Ar). ^{13}C NMR: δ (ppm) 53.80, 68.71, 70.12, 118.07, 131.50, 140.43, 157.03, 160.29, 171.18. ESI-TOF MS: m/z [M^+] calcd for $C_{52}H_{64}N_{12}S_4I_4Zn$: 1558.9730; found [$M^+$] 1558.9808.

4.1.13. 1,8(11),15(18),22(25)-Tetrakis[(2-trimethylammonium) ethylsulfanyl]phthalocyaninatozinc(II) tetraioidide (**14**) [21,22]

This compound was prepared from **10** by applying the procedure described for **13**. Yield 0.043 g (91%). IR (KBr, cm^{-1}): 2929, 1620, 1474, 1385, 1315, 1107, 898, 742. ^1H NMR (DMSO-d_6, 500 MHz): δ (ppm) 2.41 (br s, 36H, CH_3), 3.15 (m, 8H, CH_2N), 4.17 (m, 8H, SCH_2), 7.13–8.02 (m, 12H, Ar). ^{13}C NMR: δ (ppm) 53.80, 71.05, 121.98, 133.34, 151.08, 160.52, 172.03. ESI-TOF MS: m/z [M^+] calcd for $C_{52}H_{64}N_{12}S_4I_4Zn$: 1558.9730; found [$M^+$] 1558.9808.

4.2. Photophysical studies

Absorption and emission spectra were recorded at different concentrations employing a 10 × 10 mm quartz cuvette. All experiments were performed at room temperature. Compounds **7**–**10** were measured in THF and **11**–**14** in DMF and water.

The emission spectra of **7**, **9**, **11**, **13** were collected at an excitation wavelength of 610 nm (Q-band) and recorded between 630 and 800 nm whereas **8**, **10**, **12**, **14** were collected at an excitation wavelength of 630 nm and recorded between 650 and 850 nm.

Fluorescence quantum yields (Φ_F) were determined by comparison with those of tetra-*t*-butylphthalocyaninatozinc (II) ($\Phi_F = 0.30$ in toluene) as a reference at $\lambda_{exc} = 610$ nm for **7**, **9**, **11**, **13** and $\lambda_{exc} = 630$ nm for **8**, **10**, **12**, **14** [26].

Standard chemical monitor bleaching rates were used to calculate the quantum yield of singlet oxygen generation rates [54]. For Φ_Δ studies in organic solvent, DPBF was used as a singlet oxygen chemical quencher. To avoid chain reactions induced by DPBF in the presence of singlet oxygen, the absorbance of DPBF was kept under 1.9. DPBF decay at 410 nm was monitored. For Φ_Δ studies in aqueous media, singlet oxygen monitor solutions composed of imidazol (8 mM) and N,N-diethyl-4-nitrosoaniline (40–50 μM), were air saturated and irradiated. The bleaching of nitrosoaniline was followed spectrophotometrically at 440 nm as a function of time. Polychromatic irradiation was performed by using a projector lamp (Philips 7748SEHJ, 24 V–250 W) and a cut-off filter at 610 nm (Schott, RG 610) and a water-filter were used to prevent ultraviolet and infrared radiation. Samples **7**–**14** and references 2,3,9,10,16,17,23,24-octakis[(N,N-dimethylaminoethylsulfanyl)]phthalocyaninatozinc(II) (Φ_Δ = 0.69 in DMF) [31], ZnPc (Φ_Δ = 0.70 in THF) [33] and MB ($\Phi_\Delta = 0.56$ in water) [55] were irradiated within the same wavelength interval λ_1–λ_2, and Φ_Δ was calculated according Amore et al. [56].

The photo-stability of phthalocyanines **11**–**14** was determined by the decay of the Q-band intensity after exposure to red light [55] The fluence rate was adjusted to 20 mW cm^{-2}. Measurements were performed under air in water. Photodegradation rate constants k were calculated as described elsewhere [57].

4.3. Biological studies

4.3.1. Cells and culture conditions

Human nasopharynx carcinoma KB cells (ATCC CCL-17) were maintained in Minimum Essential Medium (MEM, Gibco BRL) containing 10% (v/v) fetal bovine serum (FBS, Gibco BRL), 2 mM L-glutamine, 50 U/mL penicillin, 50 μg/mL streptomycin, 1 mM sodium pyruvate and 4 mM sodium bicarbonate, in a humidified atmosphere of 5% CO_2 at 37 °C.

4.3.2. Dark cytotoxicity and photocytotoxicity

KB cells were plated at a density of 1×10^4 cells/well in 96-well microplates and incubated overnight at 37 °C until 70–80% of confluence. Cationic phthalocyanines **11**–**14** were diluted in a culture medium containing 4% FBS to give a 10 μM concentration. 2-Fold serial dilutions were then prepared and the cells were incubated for 24 h. Compounds were then removed, a complete

fresh culture medium was added and cells were exposed to a light dose of 4.7 J cm^{-2}, 1.96 mW cm^{-2} with a 150 W halogen lamp equipped with a 10 mm water-filter to maintain cells cool and attenuate IR radiation. In addition, a cut-off filter was employed to bar wavelengths shorter than 630 nm. In parallel, non-irradiated cells were used to study dark cytotoxicity. Following treatment, cells were incubated for an additional 24 h period and cell viability was determined by means of MTT reduction assay (Mosmann, 1983) [58]. Briefly, 100 μg of MTT tetrazolium salt were added and incubated for 4 h at 37 °C. Formazan crystals were solubilized in 0.01 M HCl in isopropyl alcohol and the absorbance (595 nm) was measured in a Biotrack II Microplate Reader (Amersham Biosciences). Different light doses were also employed to evaluate the cytotoxic effect of **13**. Irradiation of cells in the absence of **13** did not modify cell viability (data not shown).

4.3.3. Time-dependent cellular uptake

KB cells (1×10^4 cells/well) were grown overnight at 37 °C on 96-well microplates. A 10 μM solution of **13** in culture medium with 4% FBS was then exposed to cells from 30 min to 24 h in the dark. After incubation, cells were washed with phosphate-buffer saline (PBS) and solubilized in 100 μL/well of N,N-dimethylformamide. Drug cellular uptake was measured by determining the fluorescence emission of **13** with an SLM-Aminco Bowman Series 2 Spectrofluorometer (Spectronic Instruments, Rochester, NY) at 680 nm excitation and 688 nm emission wavelengths. Results were expressed as the emission relative to the total number of cells.

4.3.4. Intracellular localization

KB cells grown on coverslips were incubated with a 10 μM solution of **13** for 24 h at 37 °C in the dark. After removing the compound with PBS, cells were stained with the following fluorescent dyes for specific organelles diluted in the culture medium without FBS: LysoTracker Green DND-26 (75 nM, 30 min) was used to reveal lysosomes, and MitoTracker Green FM (100 nM, 45 min), to visualize mitochondrias. Both organelle dyes were obtained from Invitrogen. After washing with PBS, coverslips were fixed for 5 min at room temperature with 4% paraformaldehyde and cells were then examined by fluorescence with a confocal microscopy Olympus FV 300. Phthalocyanine **13** was excited at 633 nm and its emission was monitored at wavelengths >660 nm, and the organelles (lysosomes and mitochondrias) were excited at 488 nm and green fluorescence was detected at 510–530 nm. To examine the localization of compound **13** after irradiation, cells treated as described above were exposed to a light dose of 4.7 J cm^{-2}, and then incubated for an additional 3 h previous to fixation.

4.3.5. Caspase activity assay

After incubating KB cells for 24 h with a 5 μM solution of **13**, cells were washed and then irradiated with a light dose of 4.7 J cm^{-2} as previously described. Cells were then incubated for different time-periods at 37 °C and 1×10^6 cells were lysed for 30 min at 4 °C in 50 μL of lysis buffer (10 mM HEPES, pH 7.4, 50 mM NaCl, 2 mM $MgCl_2$, 5 mM EGTA, 1 mM PMSF, 2 μg/mL leupeptin, 2 μg/mL aprotinin) followed by three cycles of rapid freezing and thawing. Cell lysates were centrifuged at 17,000*g* for 15 min and total protein concentration was determined using Bradford reagent (Bio-Rad, Hercules, CA, U.S.A.). Aliquots containing 100 μg of protein were diluted in assay buffer (20 mM HEPES, 132 mM NaCl, 6 mM KCl, 1 mM $MgSO_4$, 1.2 mM K_2HPO_4, pH 7.4), 20% glycerol, 5 mM DTT, and incubated at 37 °C for 2 h with 50 μM of the corresponding fluorogenic substrate for caspase-3 (Ac-DEVD-AMC). Cleavage of the substrate was monitored by AMC release in a SFM25 Konton Fluorometer at 355 nm excitation and 460 nm emission wavelengths. Results were expressed as the change in fluorescence units (per μg of protein) in relation to control. Non-irradiated cells exposed or not to **13** and irradiated cells without **13** were treated as described above and included as controls.

4.3.6. Western blot analysis

KB cells were incubated during 24 h with a 5 μM solution of **13**, then washed with PBS and exposed to a light dose of 4.7 J cm^{-2} as described above. After irradiation, cells were incubated for different time-periods at 37 °C and then, 1×10^6 cells were lysed for 30 min at 4 °C in a 10 μL lysis buffer (10% glycerol, 0.5% Triton X-100, 1 μg/mL aprotinin, 1 μg/mL trysin inhibitor, 1 μg/mL leupeptin, 10 mM $Na_4P_2O_7$, 10 mM NaF, 1 mM Na_3VO_4, 1 mM EDTA, 1 mM PMSF, 150 mM NaCl, 50 mM Tris, pH 7.4). Clear cell lysate supernatants were prepared by centrifugation and aliquots containing 100 μg of protein were resuspended in 0.063 M Tris/HCl, pH 6.8, 2% SDS, 10% glycerol, 0.05% bromophenol blue, 5% 2-ME, submitted to 8% SDS-PAGE and then transferred to nitrocellulose membranes (Amersham Biosciences, Piscataway, NY, U.S.A.) for 1 h at 100 V in 25 mM Tris, 195 mM glycine, 20% methanol, pH 8.2. After blocking non-specific antibody binding sites with 10 mM Tris, 130 mM NaCl and 0.05% Tween 20, pH 7.4, (TBS-T), containing 3% bovine seralbumin (BSA), membranes were incubated overnight at 4 °C with polyclonal antibody anti-PARP (Santa Cruz Biotechnology, CA, U.S.A.) diluted in TBS-T, containing 1% BSA. Bound antibodies were revealed with anti-rabbit IgG (horseradish peroxidase-conjugated goat IgG from Santa Cruz Biotechnology, CA, U.S.A.) diluted in TBS-T, 1% BSA. Immunoreactive proteins were visualized using the ECL detection system (Amersham Biosciences, Piscataway, NY, U.S.A.) according to the manufacturer's instructions. For quantification of band intensity, Western blots were scanned with a densitometer (Gel Pro Analyzer 4.0). Non-irradiated cells exposed or not to **13** and irradiated cells without **13** were included as controls.

Acknowledgments

This work was supported by grants from the University of Buenos Aires, the Consejo Nacional de Investigaciones Científicas y Técnicas (CONICET) and the Agencia Nacional de Promoción Científica y Tecnológica. We wish to thank the technical assistance as regards chromatography of Ms. Juana Alcira Valdez. ESI-TOF mass spectrometry assistance of Mr. Diego Cobice is also appreciated as well as language supervision by Prof. Rex Davis.

References

[1] T.J. Dougherty, C.J. Gomer, B.W. Henderson, G. Jori, D. Kessel, M. Korbelik, J. Moan, Q. Peng, J. Natl. Cancer Inst. 90 (1998) 889–905.
[2] L.B. Josefsen, R.W. Boyle, Br. J. Pharmacol. 154 (2008) 1–3 (and references therein).
[3] S.M. Fien, A.R. Oseroff, J. Natl. Compr. Canc. Netw. 5 (2007) 531–540 (and references therein).
[4] R.K. Pandey, J. Porphyrins Phthalocyanines 4 (2000) 368–373.
[5] M.G.H. Vicente, Curr. Med. Chem. Anticancer Agents 1 (2001) 175–194.
[6] H. Ali, J.E. van Lier, Chem. Rev. 99 (1999) 2379–2450.
[7] I.J. MacDonald, T.J. Dougherty, J. Porphyrins Phthalocyanines 5 (2001) 105–129.
[8] M.R. Detty, S.L. Gibson, S.J. Wagner, J. Med. Chem. 47 (2004) 3897–3915.
[9] C.C. Leznoff, A.B.P. Lever (Eds.), Phthalocyanines: Properties and Applications, vols. 1–4, VCH, New York, 1989, 1992, 1993, 1996.
[10] B. Paquette, R.W. Boyle, H. Ali, A.H. MacLennan, T.G. Truscott, J.E. van Lier, Photochem. Photobiol. 53 (1991) 323–327.
[11] P. Margaron, M.-J. Grégoire, V. Scasnárt, H. Ali, J.E. van Lier, Photochem. Photobiol. 63 (1996) 217–223.
[12] K. Berg, J.C. Bommer, J. Moan, Photochem. Photobiol. 49 (1989) 587–594.
[13] V.C. Colussi, D.K. Feyes, J.W. Mulvihill, Y.-S. Li, M.E. Kenney, C.A. Elmets, N. L. Oleinick, H. Mukhtar, Photochem. Photobiol. 69 (1999) 236–241.
[14] R.B. Boyle, B. Paquette, J.E. van Lier, Br. J. Cancer 65 (1992) 813–817.
[15] J.D. Miller, E.D. Baron, H. Scull, A. Hsia, J.C. Berlin, T. McCormick, V. Colussi, M. E. Kenney, K.D. Cooper, N.L. Oleinick, Toxicol. Appl. Pharmacol. 224 (2007) 290–299.
[16] R.W. Boyle, C.C. Leznoff, J.E. van Lier, Br. J. Cancer 67 (1993) 1177–1181.
[17] M. Hu, N. Brasseur, S. Zeki Yildiz, J.E. van Lier, C.C. Leznoff, J. Med. Chem. 41 (1998) 1789–1802.

[18] W. Liu, T.J. Jensen, F.R. Fronczek, R.P. Hammer, K.M. Smith, M.G.H. Vicente, J. Med. Chem. 48 (2005) 1033–1041 (and references therein).
[19] W.O. Siegl, J. Heterocycl. Chem. 18 (1981) 1613–1618.
[20] D. Salih, G. Gulay, G. Ahmet, B. Ozer, J. Coord. Chem. 38 (1996) 287–293.
[21] M. Idowo, T. Nyokong, Polyhedron 28 (2009) 416–424.
[22] L. Zhang, J. Huang, L. Ren, M. Bai, L. Wu, B. Zhai, X. Zhou, Bioorg. Med. Chem. 16 (2008) 416–424.
[23] K. Kosuga, H. Hayashi, M. Handa, Chem. Lett. (1991) 1877–1880.
[24] T.M. Keller, T.R. Price, J.R. Griffith, Synthesis (1980) 613.
[25] D. Dei, G. Chiti, M.P. De Filippis, L. Fantetti, F. Giuliani, F. Giuntini, M.G. Soncin, G. Jori, G. Roncucci, J. Porphyrins Phthalocyanines 10 (2006) 147–159.
[26] D.A. Fernández, J. Awruch, L.E. Dicelio, Photochem. Photobiol. 63 (1996) 784–792.
[27] D.A. Fernández, J. Awruch, L.E. Dicelio, J. Photochem. Photobiol. B, Biol. 41 (1997) 227–232.
[28] M.J. Stillman, T. Nyokong, Absorption and magnetic circular dichroism spectral properties of phthalocyanines. Part 1: complexes of the dianion Pc (-2). in: C.C. Leznoff, A.B.P. Lever (Eds.), Phthalocyanines: Properties and Applications. VCH, New York, 1989, pp. 133–289.
[29] N. Kobayashi, N. Sasaki, Y. Higashi, T. Osa, Inorg. Chem. 34 (1995) 1636–1637.
[30] N. Kobayashi, H. Ogata, N. Nonaka, E.A. Luk'yanets, Chem. Eur. J. 9 (2003) 5123–5134.
[31] C.A. Strassert, G.M. Bilmes, J. Awruch, L.E. Dicelio, Photochem. Photobiol. Sci. 7 (2008) 738–747.
[32] Z.A. Bayır, Dyes Pigm. 65 (2005) 235–242.
[33] M.E. Rodriguez, F. Morán, A. Bonansea, M. Monetti, D.A. Fernández, C. A. Strassert, V. Rivarola, J. Awruch, L.E. Dicelio, Photochem. Photobiol. Sci. 2 (2003) 988–994.
[34] D. Wöhrle, N. Iskander, G. Graschew, H. Sinn, E.A. Friedrich, W. Maier-Borst, J. Stern, P. Schlag, Photochem. Photobiol. 51 (1990) 351–356.
[35] N.B. Rumie Vittar, C.G. Prucca, C.A. Strassert, J. Awruch, V. Rivarola, Int. J. Biochem. Cell Biol. 40 (2008) 2192–2205.
[36] H. Li, T.H. Jensen, F.R. Fronczek, M.G.H. Vicente, J. Med. Chem. 51 (2008) 502–511 (and references therein).
[37] D. Kessel, R. Luguya, M.G.H. Vicente, Photochem. Photobiol. 78 (2003) 431–435.
[38] D. Kessel, Y. Luo, J. Porphyrins Phthalocyanines 5 (2001) 181–184.
[39] M.O. Hengartner, Nature 407 (2000) 770–776.
[40] H. Kaufmann, M.O. Hengartner, Trends Cell Biol. 11 (2001) 526–534.
[41] D.R. Green, J.C. Reed, Science 281 (1998) 1309–1312.
[42] N.A. Thornberry, Y. Lazebnik, Science 281 (1998) 1312–1316.
[43] M.G. Grutter, Curr. Opin. Struct. Biol. 10 (2000) 649–655.
[44] N.N. Danial, S.J. Korsmeyer, Cell 116 (2004) 205–219.
[45] A. Rodríguez-Hernández, G. Brea-Calvo, D.J. Fernández-Ayala, M. Cordero, P. Navas, J.A. Sánchez-Alcáza, r, Apoptosis 11 (2006) 131–139.
[46] P.O. Hassa, S.S. Haenni, M. Elser, M.O. Hottiger, Microbiol. Mol. Biol. Rev. 70 (2006) 789–829.
[47] P.O. Hassa, M.O. Hottiger, Front. Biosci. 13 (2008) 3046–3082.
[48] D. Kessel, Y. Luo, P. Mathieu, J.J. Reiners Jr., Photochem. Photobiol. 71 (2000) 196–200.
[49] P. Boya, R.A. Gonzalez-Polo, D. Poncet, K. Andreau, H.L. Vieira, T. Roumier, J.L. Perfettini, G. Kroemer, Oncogene 22 (2003) 3927–3936.
[50] M.E. Guicciardi, M. Leist, G.J. Gores, Oncogene 23 (2004) 2881–2890.
[51] C. Tardy, P. . Codogno, H. Autefage, T. Levade, N. Andrieu-Abadie, Biochim. Biophys. Acta 1765 (2006) 101–125.
[52] P. Boya, G. Kroemer, Oncogene 27 (2008) 6434–6451.
[53] D.R. Burfield, R.H. Smithers, J. Org. Chem. 43 (1978) 3966–3968.
[54] M.G. Lagorio, L.E. Dicelio, E. San Roman, J. Photochem. Photobiol. A: Chem. 72 (1993) 153–161.
[55] F. Wilkinson, W.P. Helman, A.B. Ross, J. Phys. Chem. Ref. Data 24 (1995) 663–1021.
[56] S. Amore, M.G. Lagorio, L.E. Dicelio, E. San Román, Prog. React. Kinet. Mech. 26 (2001) 159–177.
[57] G. Schnurpfeil, A.K. Sobbi, W. Spillger, H. Kliesch, D.J. Wöhrle, J. Porphyrins Phthalocyanines 1 (1997) 159–167.
[58] T. Mosmann, J. Immunol. Methods 65 (1983) 55–63.